

Article

Egg Morphology and Chorionic Ultrastructure of Spotted Lanternfly, *Lycorma delicatula* (White) (Hemiptera: Fulgoridae)

Jonathan M. Powell ¹, Laura J. Nixon ² , Austin P. Lourie ³, Tracy C. Leskey ² and Spencer S. Walse ^{1,3,*} 

- ¹ United States Department of Agriculture, Agricultural Research Service, San Joaquin Valley Agricultural Sciences Center, 9611 South Riverbend Avenue, Parlier, CA 93648, USA
- ² United States Department of Agriculture, Agricultural Research Service, Appalachian Fruit Research Station, 2217 Wiltshire Rd., Kearneysville, WV 25430, USA
- ³ Agricultural and Environmental Chemistry Graduate Group, Department of Environmental Toxicology, University of California at Davis, 4117 Meyer Hall, Davis, CA 95616, USA
- * Correspondence: spencer.walse@usda.gov; Tel.: +1-559-596-2750

Abstract: Knowledge regarding egg morphology can aid the selection of postharvest fumigants for insect control. Accordingly, scanning electron microscopy (SEM) was used to examine eggs of spotted lanternfly (SLF), *Lycorma delicatula* (White) (Hemiptera: Fulgoridae), a pest recently invasive to the mid-Atlantic region of the United States. As the overwintering life stage of SLF, eggs are deposited on a variety of refugia, including many forestry products that can be distributed geographically via travel, commerce, and/or trade. For fumigation to control SLF, and potentially translate into a viable strategy for limiting the spread of SLF by subject pathways, the fumigant must permeate the chorion to react with biomolecules and/or disrupt cellular processes. SLF chorion was characterized by a porous network of aeropyles localized around the operculum, in cranial and caudal relation to the developing nymph, as well as an interstice between the operculum edge and the opercular rim. The confirmation of chorionic ultrastructure that allows for ready gas exchange warrants further investigation of fumigation efficacy, even for those “non-reactive” fumigants, such as phosphine and hydrogen cyanide, which must overcome the suppression of cellular processes coincident with overwintering.

Keywords: spotted lanternfly; chorion; egg respiration; aeropyles



Citation: Powell, J.M.; Nixon, L.J.; Lourie, A.P.; Leskey, T.C.; Walse, S.S. Egg Morphology and Chorionic Ultrastructure of Spotted Lanternfly, *Lycorma delicatula* (White) (Hemiptera: Fulgoridae). *Forests* **2023**, *14*, 2354. <https://doi.org/10.3390/f14122354>

Academic Editors: Bert Cregg and Cate Macinnis-Ng

Received: 20 September 2023
Revised: 11 November 2023
Accepted: 23 November 2023
Published: 30 November 2023



Copyright: © 2023 by the authors. Licensee MDPI, Basel, Switzerland. This article is an open access article distributed under the terms and conditions of the Creative Commons Attribution (CC BY) license (<https://creativecommons.org/licenses/by/4.0/>).

1. Introduction

Spotted lanternfly (SLF), *Lycorma delicatula* White (Hemiptera: Fulgoridae), is a polyphagous fulgorid invasive to the United States (U.S.). First detected in Berks County, Pennsylvania, during 2014, SLF has since spread to, and established in, numerous states including Pennsylvania, New Jersey, New York, North Carolina, Connecticut, Maryland, Delaware, Virginia, and West Virginia [1–3]. SLF has a broad host range, with over 100 host plant species reported globally, including significant agricultural, ornamental, and forestry plants [4–6].

Spotted lanternflies are univoltine, they overwinter as egg masses that hatch into nymphs in spring, four nymphal instars develop throughout the summer, and adults begin to emerge in midsummer [5,7]. Adult populations are observed throughout the fall, with courtship and egg laying peaking during late October in the mid-Atlantic region of the U.S. These populations decline and generally die off by December with cold weather [5]. Overwintering egg masses pose the greatest concern to importers of articles from the mid-Atlantic region, as SLFs lay eggs on available various solid surfaces, which can include forest products such as logs, bark, sawn timber, Christmas trees, nursery plants, patio furniture, timber dunnage and packaging, pallets, construction materials, and many others [3]. SLF is also of concern to U.S. horticultural producers, as it has the potential to serve as a barrier to interstate and foreign exports. In the context of limiting the spread of SLF, research was

initiated to identify efficacious phytosanitary treatments that can be applied to articles prior to movement from infested areas, or upon arrival into an area not yet infested. While efforts continue across the gamut of postharvest strategies (e.g., cold-treatments, heat-treatments, irradiation, controlled-atmosphere, fogging, etc.), fumigation remains an invaluable option for insect pest control.

Postharvest fumigants are generally categorized into two groups, those that are delivered in a form that must “react” with biomolecules and/or matter to elicit toxicity, or those that are a “non-reactive”, being delivered as the toxicant. With respect to “reactive” fumigants, methyl bromide and propylene oxide alkylate nitrogen- and sulfur-containing biomolecules [8,9], sulfuryl fluoride must be hydrolyzed to yield fluoride ions that inhibit glycolysis [10–12], and ethyl formate also must be hydrolyzed to yield formate, which is a cytochrome C oxidase inhibitor [13–16]. Methyl bromide, Metho-O-Gas 100[®], is registered in the U.S. to treat a variety of nonfood products, including logs and lumber, forest and plant products, and miscellaneous cargo. The use of methyl bromide is ultimately left to the discretion of the importing party or country [17]. Methyl bromide use is regulated under the Montreal Protocol, where Decision XX/6 by the Methyl Bromide Technical Options Committee (MBTOC) recognizes “that methyl bromide use for quarantine and pre-shipment (QPS) purposes is an important remaining use of an ozone-depleting substance that is not controlled pursuant to paragraph 6 of Article 2H” [18]. Decision VII/5 of MBTOC “urges Parties to refrain from using methyl bromide and to use nonozone depleting technologies wherever possible”. Sulfuryl fluoride is also registered in the U.S., with Vikane[®] and Profume[®] labels listing numerous products that could serve as harborage for SLF eggs. Numerous reports indicate sulfuryl fluoride is generally more toxic than methyl bromide toward postembryonic life stages of a given insect species [19]. However, insect eggs are more tolerant toward sulfuryl fluoride, often requiring many times the dosage required to control adults of the same species [20,21]. Propylene oxide and ethyl formate are not currently registered in the U.S. to treat subject articles; however, both have been recognized as potent fumigants with ovicidal potential [22].

With respect to the “non-reactive” fumigants, hydrogen cyanide poisons the mitochondrial electron transport chain within cells by binding to the a3 portion (complex IV) of cytochrome c oxidase, and several studies indicate phosphine also inhibits cytochrome c oxidase activity [23–25]. However, multiple pathways are involved with phosphine toxicity, as evidenced by the “narcosis threshold” in the seminal works of Winks and Waterford [26] and discussed as the “sweet spot” in works of Walse et al. (2021) [27] and Lampiri et al. (2021) [28]. Phosphine is registered in the U.S., in metal phosphide and cylinderized formulations, to treat many types of construction materials and wood products. While extremely versatile, preparations should be made to minimize the potential for phosphine-catalyzed corrosion of metals that may damage articulates [29]. Hydrogen cyanide is not currently registered in the U.S., yet it has a long history of use in targeting insects, including eggs [30].

Regardless of the mechanism or mode of action, fumigant efficacy increases as temperature, and in turn insect activity, increases. The key distinction, though, between these groups of fumigants is that the “reactive” fumigants can react, do cellular damage when the insect is not active, and then toxicity is imparted when activity resumes. Whereas, if a fumigation with a “non-reactive” fumigant is conducted when the insect is not active, there is a risk that opportunity for toxicity will be lost. It should also be noted that in general, phosphine and hydrogen cyanide are inexpensive relative to the “reactive” fumigants, so their use is of economic interest.

The egg is generally recognized as the most fumigant-tolerant life stage of insects, at least with respect to the fumigants cited above [31–36]. The influence of abiotic factors such as temperature, exposure time, pressure, and concentration on ovicidal efficacy of fumigants has been well documented across many insect species and in general, the functional and operational parameters have been identified for each fumigant [21,37,38]. The differential response of species to the same fumigant is critically linked to a variety of biotic factors; however, including the structure and composition of the egg chorion as related to fumigant

permeability, and developmental rate, a proxy for cellular/metabolic activity required for fumigant activity (e.g., glycolysis inhibition, electron transport inhibition, etc.) [39–45].

Much uncertainty surrounds the potential efficacy of fumigants toward SLF eggs. Understanding the relative developmental activity across the overwintering period could prove insightful, particularly for the “non-reactive” fumigants, as suppressed metabolic activity in wintertime typically decreases fumigation efficacy. However, first and foremost, fumigants must be able to access biological material within the egg. We report the abundance, distribution, and location of openings in the chorion of SLF eggs, through which fumigants can pass. Results are discussed in the context of providing industry a means for complying with existing and future quarantines that regulate the movement of SLF-free forestry products from infested areas, in the event certain articles or pathways are identified to require fumigation. With respect to the marketing of Christmas trees, growers in the mid-Atlantic region are working closely with State and Federal regulators to ensure quarantine requirements are met prior to sale, including participation in integrated pest management (IPM) training sessions that minimize the potential movement of this pest. This research seeks to identify if fumigation can further the IPM effort directly, by controlling SLF eggs in harvested Christmas trees, and/or indirectly by controlling SLF in other articles that impact Christmas tree shipping and marketing.

2. Materials and Methods

2.1. Egg Collection

Spotted lanternfly eggs were collected over the course of 7 days in November 2021 from SLF-infested sites located in Frederick County, Virginia, by carefully removing sections of bark from trees and logs on which individual egg masses were laid. Egg masses remained on the bark substrate, “backing”. Each bark backing/egg mass was placed into a ~110-mL clear plastic “snap cap” cage modified with 8 mm diameter stainless-steel 100 wire mesh gas-portals on the bottom, snap cap, and side. A paper tissue was inserted into the cage to immobilize the egg mass, with the intent of preventing jarring during handling and/or shipping.

Cages were gathered, randomly assembled into three groupings of roughly 300 cages, and stored in a shed under ambient atmospheric conditions at Fort Collier Civil War Center, Winchester, Virginia, U.S. (39°12'4" N 78°9'13" W). Air temperature and relative humidity (RH) within the shed were measured cumulatively over the duration of storage by a probe (U12-015-02, Onset HOBO Data Loggers, Melrose, Massachusetts, U.S.) with a 10 min scanning/sampling rate, and yielded means (\bar{x}) of 13.41 °C and 37.2%, respectively. One of the three groupings was packaged and shipped on ca. 20 January 2022, per conditions of APHIS Permit P526-200621-01, to UC Davis Contained Research Facility (CRF) (University of California, Davis, California, U.S.), a BSL-III quarantine facility. An additional probe, operated analogously, was used to record respective means (\bar{x}) of 1.02 °C and 57.0% within the package over the course of shipment. Subsequent groupings were packaged and shipped as above on ca. 1 March 2022 (\bar{x} : 4.44 °C, 79.5% RH) and 5 April 2022 (\bar{x} : 12.9 °C, 47.9% RH).

Upon the arrival of each shipment to the CRF, the cages were removed from packaging and the bark backings were removed from their respective cages. To minimize potential for fungal infection, each bark backing was submerged for 60 s in an aqueous solution of potassium sorbate (5 wt%). Each bark backing was left to dry at room temperature near 25° atop a paper towel, with the egg mass facing upward. Five to six dried bark backings were transferred to a 950-mL plastic cup cage (Pro-Kal Polypropylene Clear Deli Containers, PK32TC, Greenville, South Carolina, U.S.), modified with cloth mesh gas-portals on the lid and side. The storage containers were stored in a refrigerator (Model REC4504A21, Thermo Electron Corporation, Waltham, Massachusetts, U.S.) with a set point of 3 °C and 65% RH.

2.2. Microscopy

2.2.1. Scanning Electron Microscopy

An individual egg was carefully removed from the bark backing using dissection forceps and/or a soft bristle brush (Silver Brush, Windsor, NJ, U.S.). An initial brushing was used to remove as much as possible of the ca. 1 mm layer of oothecum covering the entire egg mass, which was notably insoluble in water as well as hexane. Six eggs at a time were placed inside a 50-mL beaker filled with 30 mL of 18 M Ω ultrapure deionized water (Nanopure, APS Water Services Corp., Lake Balboa, CA, U.S.), which was sonicated (Model 8852, Cole-Parmer, Chatswood, New South Wales, Australia) for 20 min at ambient laboratory temperature. Sonicated eggs were individually gathered and then gently brushed again to remove any remaining oothecum. No anatomical changes were observed during oothecum removal, as the brushing and sonication did not deform or puncture the firm chorion. Each of two “cleaned” eggs were mounted on double-sided carbon “sticky” tabs, which were then adhered using a soft brush on an aluminum stub (Ted Pella, Inc., Redding, California, U.S.). Paired eggs were setup on opposing sides of the tab, each 4 mm from center. In order to prevent electrostatic charging of specimens and to increase secondary electron signals, eggs (or hatchlings) were sputter coated with gold (SPI Module Sputter Coater) (SPI Supplies, West Chester, Pennsylvania, U.S.) by a modified method from Gautam et al. (2014) [41,46,47]. The mounted specimens were then viewed using a scanning electron microscope (S-3500N Hitachi, High Technologies America, Pleasanton, California, U.S.) and digital images were taken at 5.00 kV.

2.2.2. Time-Lapse Light Microscopy

A bark baking with a cluster of SLF eggs was sealed inside a petri dish using thermo-plastic sealing film. The specimen was imaged using a stereo microscope (Leica MZ12.5, Leica Microsystems Inc., Deerfield, Illinois, U.S.) and images were captured using a microscope-mounted digital camera (Spot Insight 2 color mosaic camera, Spot Imaging, Sterling Heights, Michigan, U.S.). The time-lapse images were acquired with Spot Basic 5.6 software (Spot Imaging, Sterling Heights, Michigan, U.S.) using the image sequence function and images were captured at an interval of 20 s.

3. Results and Discussion

SEM was used to identify several structural features likely to afford fumigants access to the interior of the egg. In Figure 1, an entire SLF egg is shown with a distinct stem-like nodule oriented anterior to the operculum (i.e., hatch door). In all observations, the operculum was completely removed during the hatching process. The stem-like structure is likely a protruding micropylar process, commonly seen in other Hemiptera insects [48–52]. Obstruction by the oothecum prevented the identification and measurement of the micropylar channel(s), which were omitted from the calculations below. Time-lapse light microscopy recorded over 50 min, spanned first movement of the operculum through complete emergence of the hatchling, and was used to establish orientation of the developing nymph for spatial reference (Supplementary Video S1). An anterior view of the hatchling’s head was then obtained with SEM (Figure 2). An SLF egg was symmetric about the sagittal plane, measuring ca. 2 mm in length and ca. 1 mm in width, but differed greatly across the coronal plane. The operculum was medially centered across the crest of a ventral concave “pinch”, whereas the dorsal region was spheroidal. This general form was observed in all specimens using both types of microscopies. Four eggs from three separate oothecae (egg masses) were examined to determine the porosity of the egg surface. The mean surface area of an egg was estimated at $1.2 \times 10^7 \pm 1.0 \times 10^5 \mu\text{m}^2$ ($\bar{x} \pm s$, $n = 4$) calculated for a prolate spheroid as:

$$SA = 2\pi\alpha\left(1 + \frac{c}{\alpha\epsilon}\arcsin\epsilon\right) \quad (1)$$

where α is the transverse radius, c is the sagittal radius, and $\epsilon^2 = (1 - \alpha^2/c^2)$.

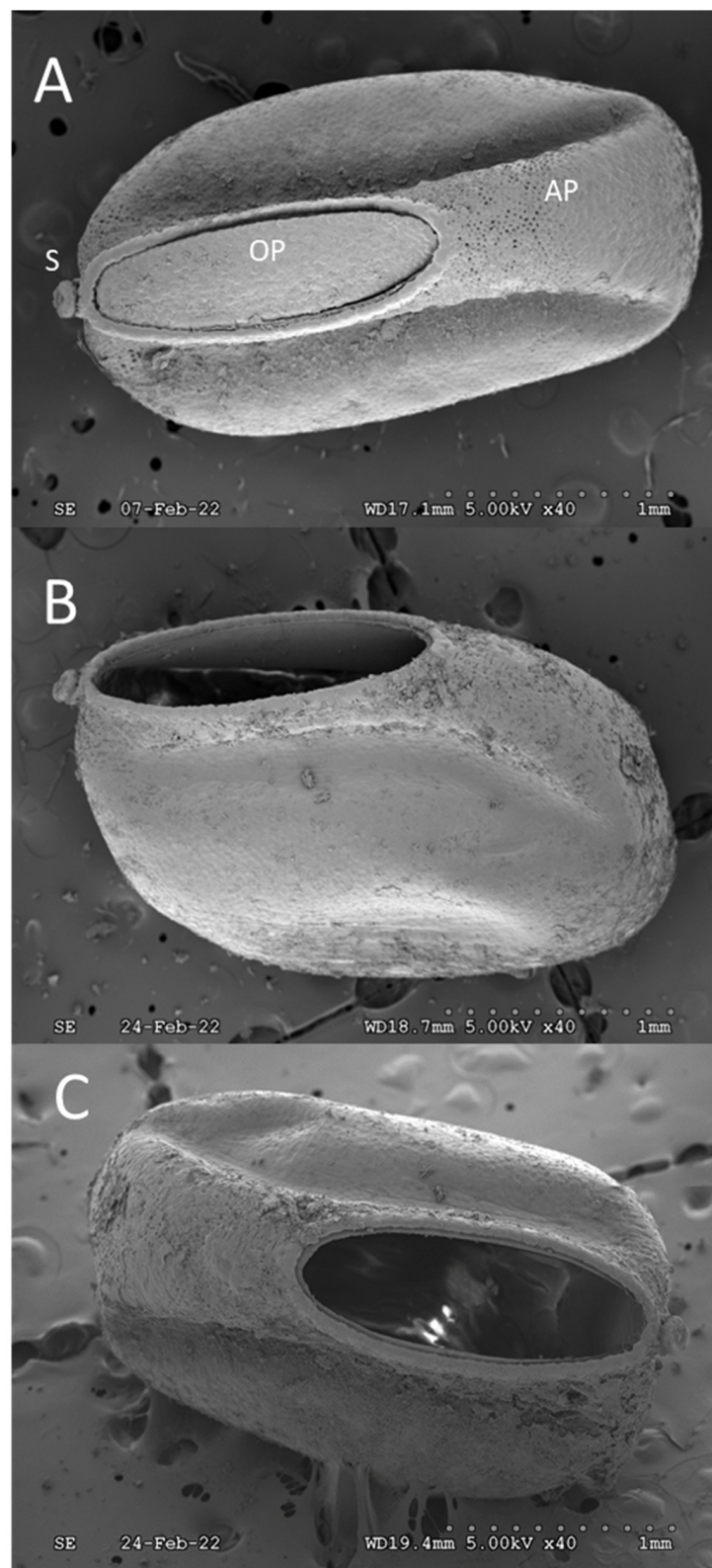


Figure 1. (A) Spotted lanternfly (SLF) (*Lycorma delicatula*) egg with operculum in place prior to hatching, (B) egg with the operculum removed after hatching, and (C) alternative ventral view of hatched SLF egg showing the vacated interior. Structures of interest labeled include the stem structure (S), operculum (OP), and aeropyles (AP).

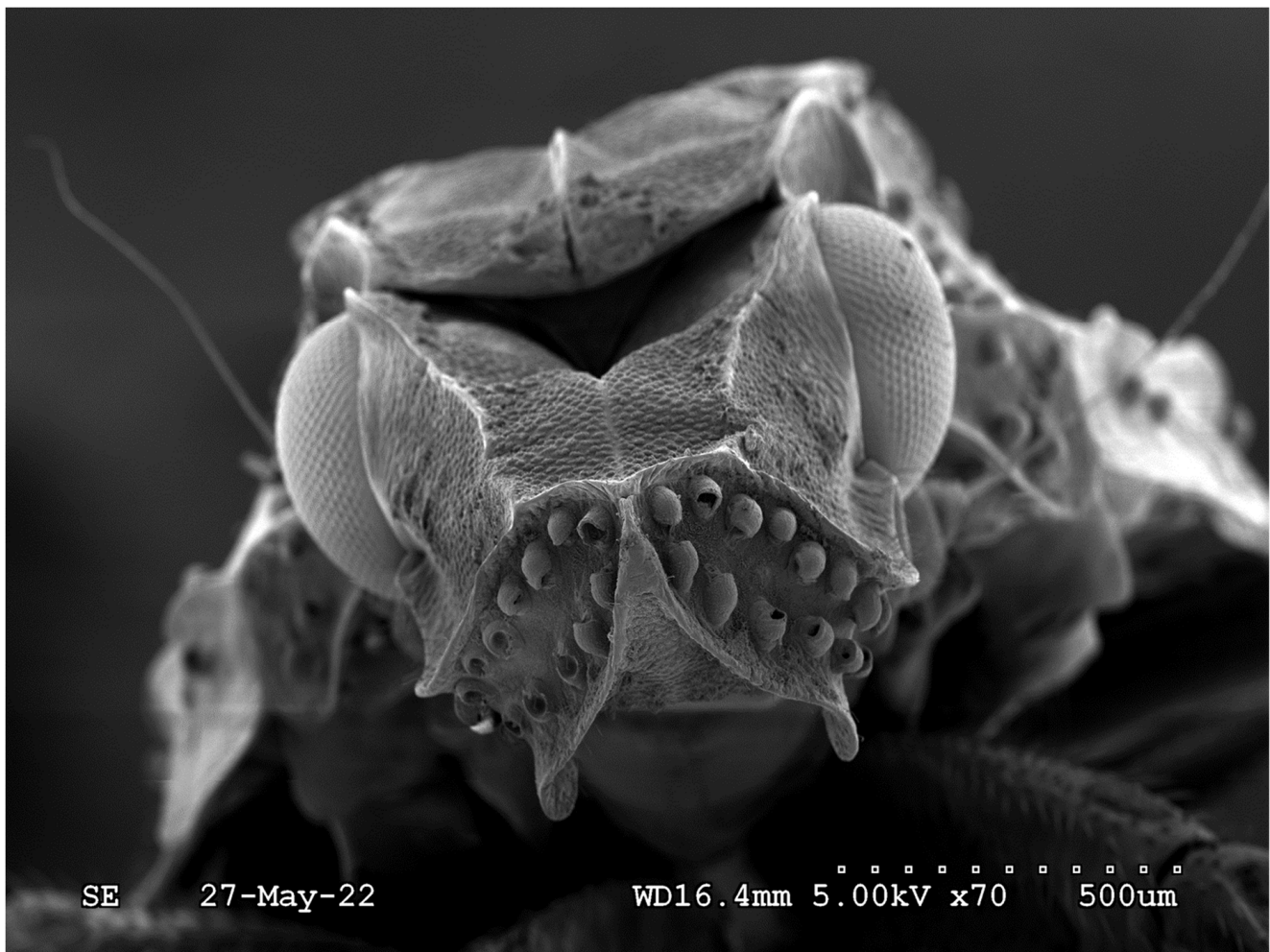


Figure 2. Anterior, frontal view of 1st instar spotted lanternfly (SLF) (*Lycorma delicatula*) imaged within hours of hatching.

A porous network of aeropyles was found on the chorion, around the operculum. The caudal area of aeropyles was localized atop the crest of the “pinch”, whereas cranial areas were localized ventrally as the “pinch” transitioned to the dorsal region (Figure 3). Expanded anterior images show that the egg surface is composed mainly of connected hexagonal plastron plates with rough regional complexity. Similar plastron structure was observed during dorsal imaging.

The stem-like nodule, shaped like a concave flowerette, was located on the anterior, ventral side of the egg at the base of the operculum (Figure 4). Unfortunately, due to the complete coverage by oothecum pores, the fine structural details were obscured. The stem-like nodule extended approximately 90 μm from the egg with an estimated diameter of $149.2 \pm 4.2 \mu\text{m}$ ($n = 4$), tilted roughly 30° from vertical, with the concave surface facing upward and away from the attachment medium. The central dome shaped protrusion had an estimated diameter of $34.1 \pm 4.1 \mu\text{m}$ ($n = 4$). It is believed that this structure serves similar purposes as other aero/micropylar processes, although no evidence of similar structures was found in the literature.

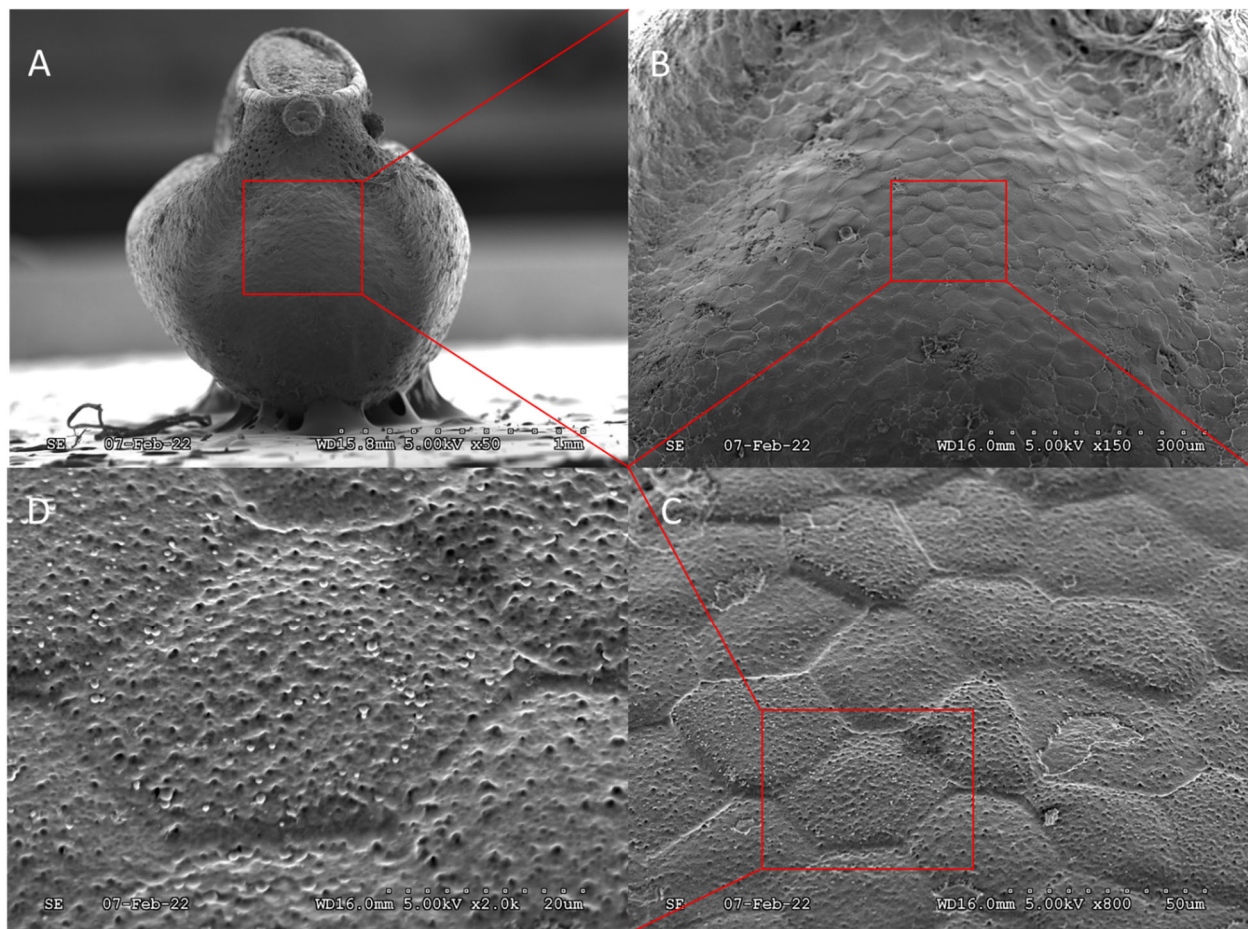


Figure 3. (A) Anterior view of a spotted lanternfly (SLF) (*Lycorma delicatula*) egg. The pinched shape of the ventral region, concave anterior surface, and also the concentric stem-like micropylar process are characteristic features. Increased magnification (B–D) of the regional complexity of the concave surface of hexagonal plastron plates.

Pores are naturally covered by oothecum, some of which were not removed during sample preparation, and are visible in Figure 5. Upon examination of a single egg, unobstructed pores were measured to a mean circular diameter of $18.9 \pm 3.4 \mu\text{m}$ ($\bar{x} \pm s$, $n = 8$). The grand mean number of pores per egg was estimated to be ca. 1600 based on the mean number of pores (14.6 ± 1.4 , $n = 6$) located in an unobstructed $110 \times 110 \mu\text{m}$ square section, multiplied by the estimated number of square sections containing pores on the egg surface, 110. Accordingly, over ca. 3% of the egg surface area, ca. $360,000 \mu\text{m}^2$, is open to gas exchange. It is interesting to note that “porosity” is >1000-fold greater than the stored product insect pests studied by Gautam et al. (2014, 2015) [41,42] and Arbogast et al. (1980) [52]. In general, at least for stored product insect pests [41,42,45], eggs from a species that take relatively long to develop have more respiratory openings compared to the eggs of a faster developing species. These previous results suggest the relative porosity of SLF chorion is associated with the balance between respiration requirements and delayed development during the 3- to 5-month-long period of overwintering. Nevertheless, the observed porosity hints at surfactant and/or oil “penetrants”, not necessarily coapplied with insecticides, as potential tools to control SLF hatching from egg masses laid on live trees, as well as forest products. The results also reinforce the interpretation that the oothecum, while gas permeable, serves a protective purpose, as its hydrophobicity deters water droplets from entering through pores.

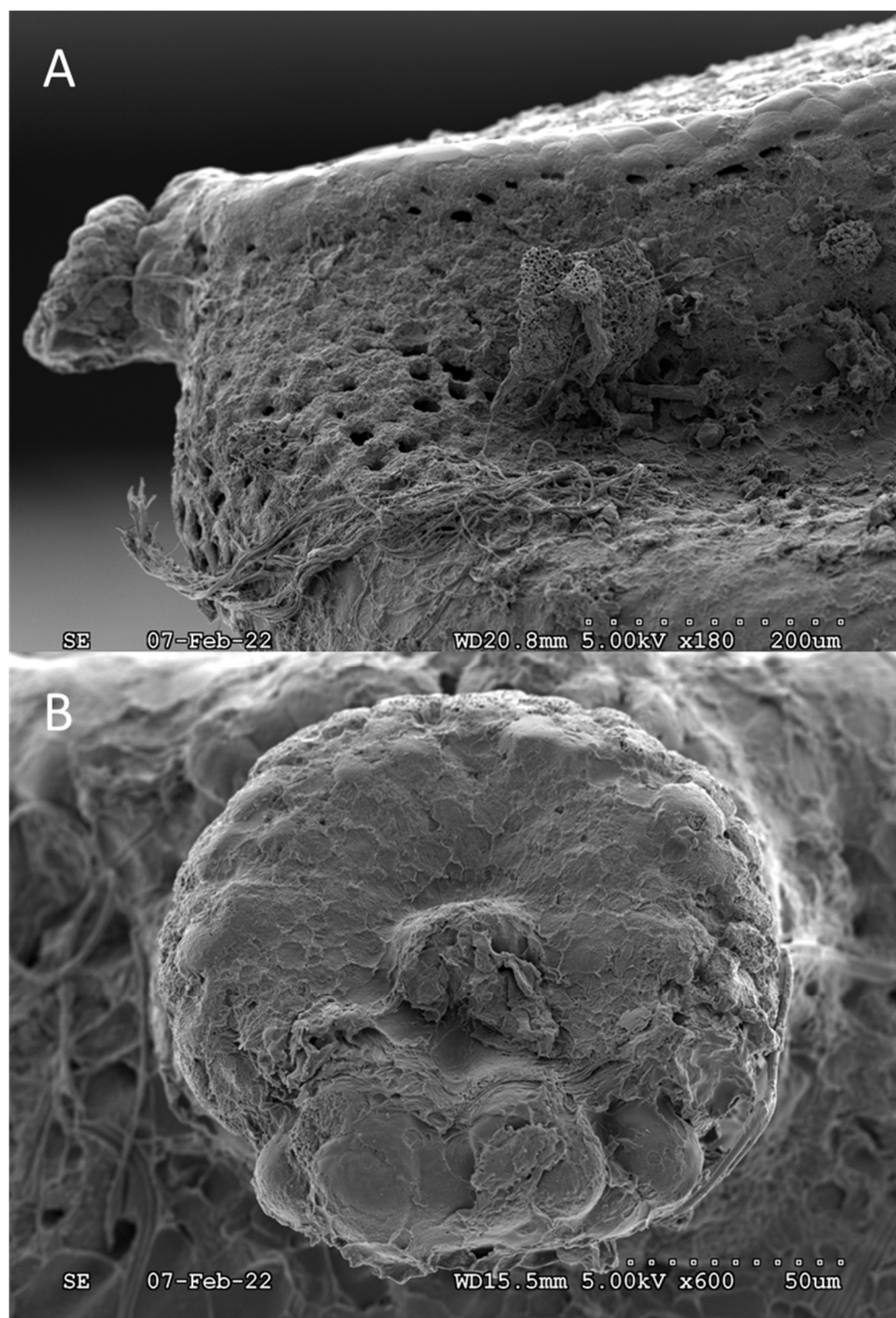


Figure 4. Stem-like nodule, presumably a micropylar process, located on the anterior ventral lip of the SLF egg, immediately adjacent to the operculum crown. **(A)** Side view showing the upward tilting angle and protrusion. **(B)** Enlarged frontal view showing hemispherical protuberance in center of the concave “flowerette”, as well as its coverage by the oothecum preventing identification of microstructures.

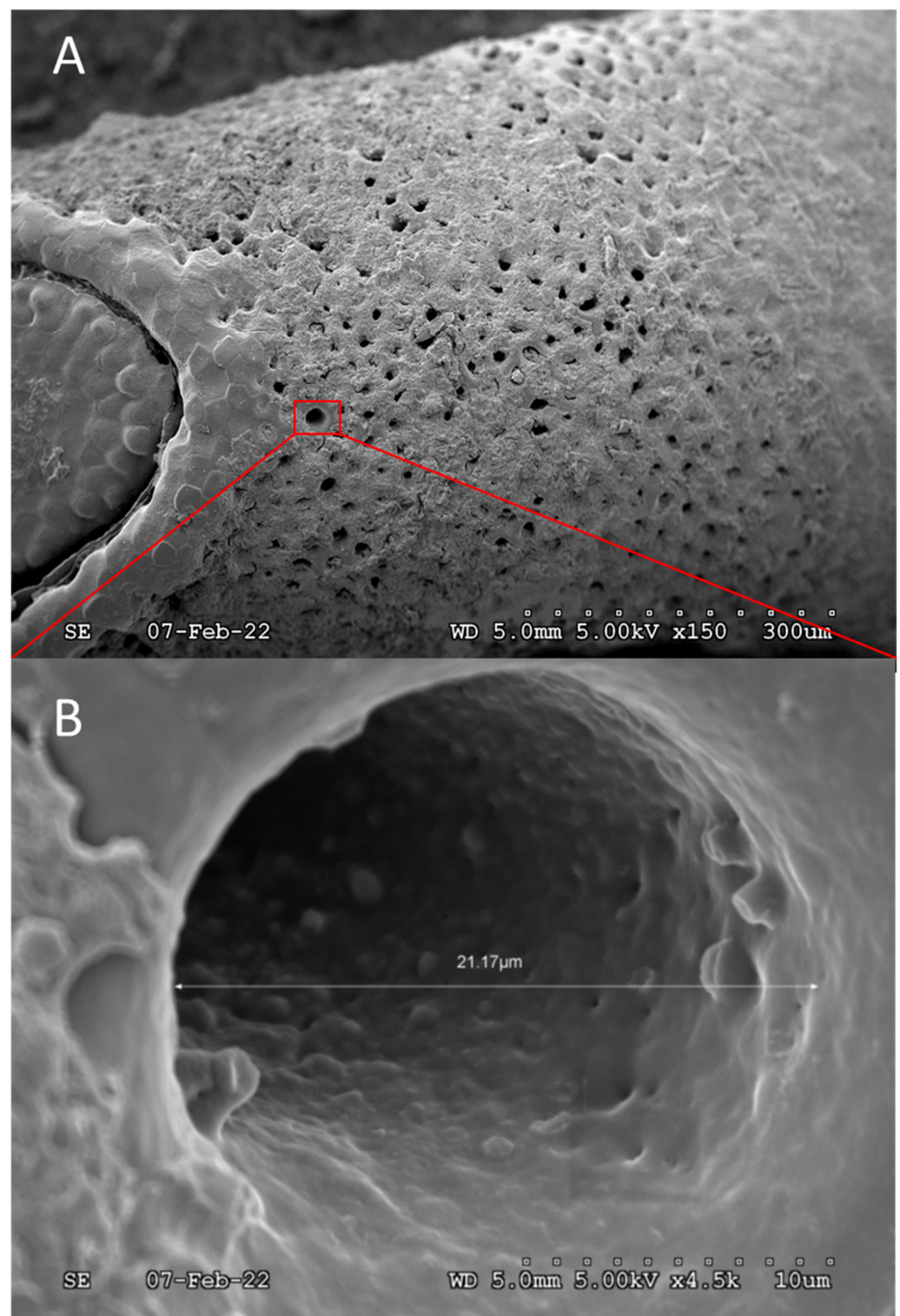


Figure 5. (A) Pores on the ventral surface, below the operculum, still partially covered by the “protective” oothecum. (B) Expanded view of a single, unobstructed pore showing general size and interior cavity.

An interstice, or small gap, was observed between the peripheral edge of the operculum and opercular rim (Figure 6). The scale of the interstice, 0 to 40 μm , provides evidence that fumigants can also diffuse into the egg interior by this route, prior to hatching, and is suggestive of only “loose” connectivity of the operculum, which was supported by the finding that no hatchlings were obstructed by “partial openings”. Microstructures were spaced along the peripheral edge of the operculum, pointing inward over the gap, presumably for defensive purposes; however, evaluating function is outside the scope of this work. The operculum and the opercular rim were examined under closer magnification after hatching (Figures 7 and 8). A distinct groove around the opercular rim is present, suggesting that this is the location that seats the operculum. A sharp contrast exists between the external lip of the groove, which appears smooth, and the internal lip, which appears much rougher in texture (Figure 7). Figure 8 shows images of the detached operculum after hatching. The exterior of the operculum is smooth in texture and lacks distinct morphological features, while the interior side of the operculum is very rough, fibrous, and spongy in appearance.

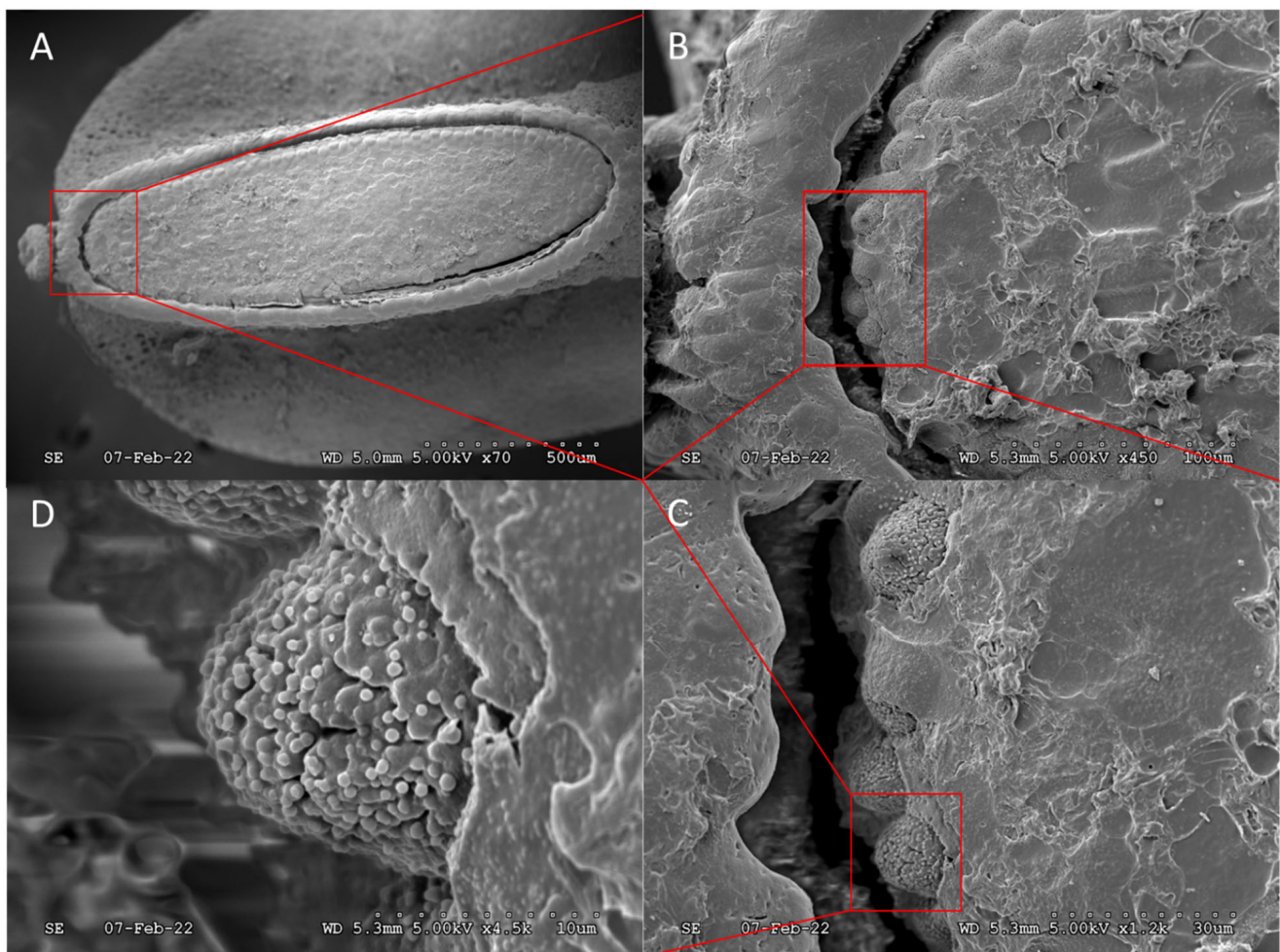


Figure 6. (A) Expanded ventral view of the operculum “hatch door”, which appears to be loosely connected, given the gaps between the operculum and rim of the egg opening. Expanded views (B–D) of the operculum “gap” featuring dome-like microstructures on the peripheral edge of the operculum.

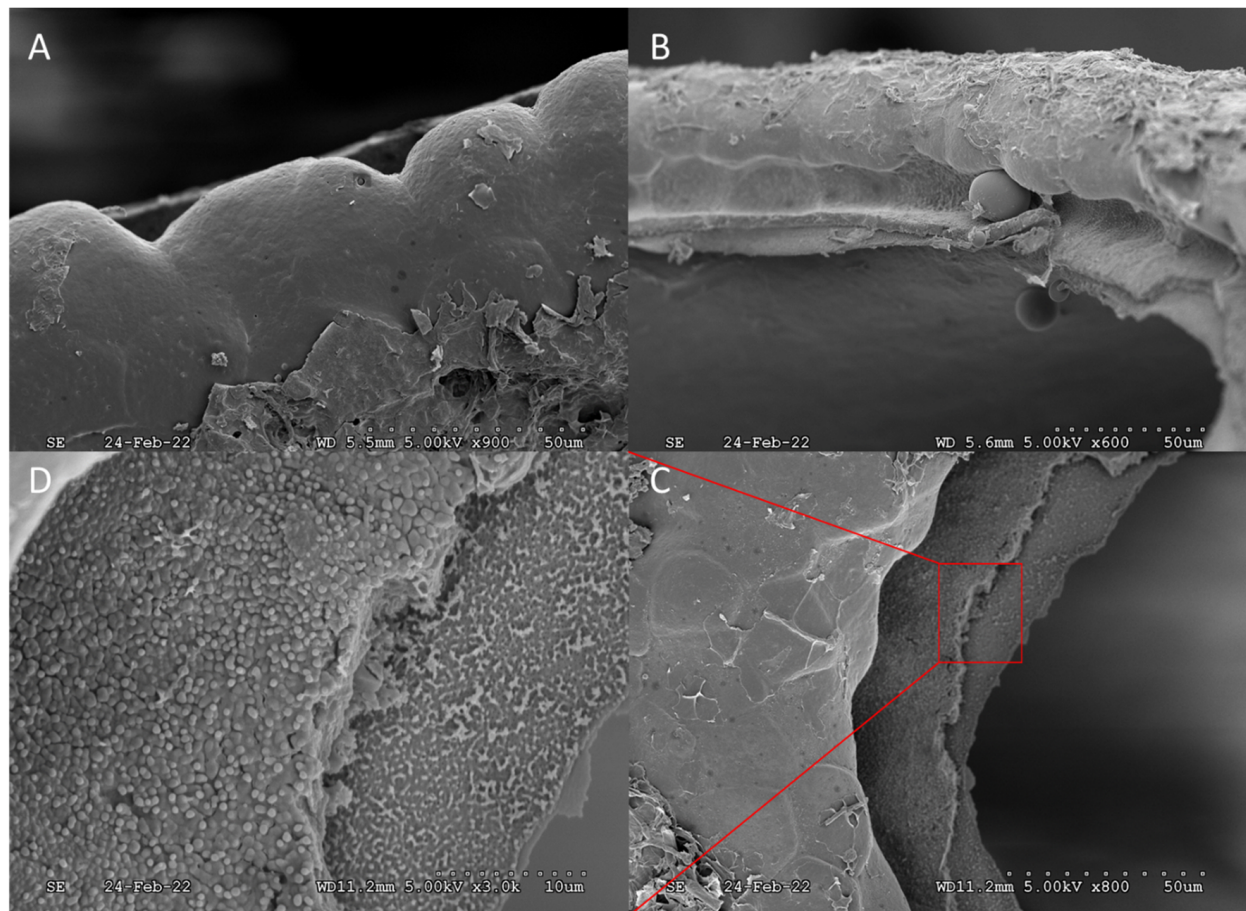


Figure 7. (A) Expanded images (A,B) of the egg rim surrounding the operculum, after hatching. Expanded images (C,D) showing difference in morphology between external and internal edges of the operculum and its connective framework.

Although the chorionic morphology can vary for a given insect species and individual, the dozens of examined chorions appeared structurally similar, with openings to allow fumigant penetration. Molecular diameter and areas of some common fumigants were tabulated (Table 1) and, in theory, billions of fumigant molecules could fit within a single pore or the operculum “gap” simultaneously. Studies are underway to define the relative ovicidal efficacy of fumigants toward SLF, and Haber’s parameters will be evaluated for each fumigant. Importantly, the results of this microscopy study indicate that all fumigants should diffuse, unobstructed, through the chorion and into the egg. While “reactive” fumigants should be effective, the effectiveness of the “non-reactive” fumigants remains uncertain, as the suppression of cellular processes coincident with overwintering may drastically decrease toxicity.

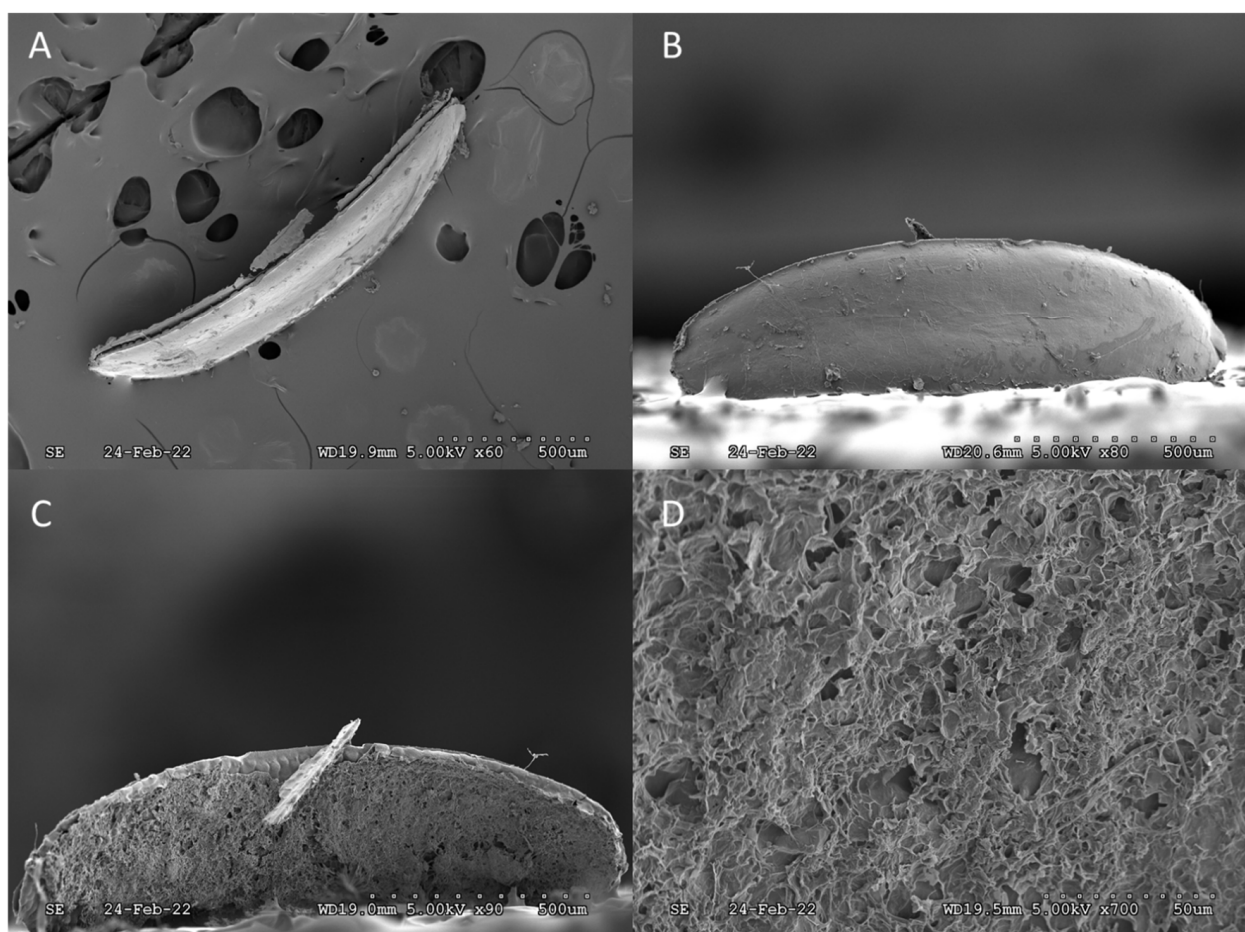


Figure 8. Views of the detached operculum “hatch door”: cross-sectional (A), exterior (B), interior (C), and (D) magnified interior image showing a rougher and more fibrous regional complexity as opposed to the smooth surface regional complexity of the exterior.

Table 1. Fumigants are expected to easily penetrate into a spotted lanternfly (SLF) (*Lycorma delicatula*) egg because the sizes of fumigant molecules are small compared to the ~18,900 nm diameter of a single pore, and there are ~1600 pores on each egg. Note, too, that the largest operculum “gap”, another route for fumigant entry, was ~40,000 nm.

Fumigant	Molecule Diameter (nm)	Molecular Area (nm ²)	# Molecules per Pore (Billions)
ethyl formate	0.557	0.2435	1.15
sulfuryl fluoride	0.259	0.0527	5.31
phosphine	0.255	0.0510	5.48
methyl bromide	0.221	0.0383	7.29
hydrogen cyanide	0.219	0.0376	7.42

4. Conclusions

These SEM results indicate for the first time that fumigants can enter SLF eggs through respiratory pores as well as the operculum “gap”. The results suggest that fumigation should be explored as a means to limit the spread of SLF by the transportation of goods that harbor egg masses. Importantly for the forestry sector, there is a profound history of coupling fumigation with the transportation and trade of logs, wood chips, bark, sawn timber, and ornamental trees, including the pine, fir, and spruce species associated with

Christmas. Once efficacious fumigation parameters have been identified, results will be transferred to registrants, fumigation service providers, and regulators for commercial implementation in the mid-Atlantic region of the U.S. and beyond as required.

Supplementary Materials: The following supporting information can be downloaded at: <https://www.mdpi.com/article/10.3390/f14122354/s1>, Video S1: Time-lapsed recording of spotted lanternfly (SLF) (*Lycorma delicatula*) (White) (Hemiptera: Fulgoridae) hatching. Video spans a period of 3000 s.

Author Contributions: Conceptualization, S.S.W.; methodology, J.M.P., L.J.N., A.P.L. and T.C.L.; software, J.M.P.; validation, J.M.P. and S.S.W.; formal analysis, J.M.P. and S.S.W.; investigation, J.M.P., A.P.L. and S.S.W.; resources, S.S.W.; data curation, J.M.P. and S.S.W.; writing—original draft preparation, J.M.P., L.J.N., A.P.L., T.C.L. and S.S.W.; writing—review and editing, J.M.P., T.C.L. and S.S.W.; visualization, J.M.P.; supervision, S.S.W.; project administration, S.S.W.; funding acquisition, S.S.W. All authors have read and agreed to the published version of the manuscript.

Funding: This research was funded by USDA-Animal Plant Health Inspection Service Plant Protection Act Section 7721 grant 10025-PPQS&T00-22-0209.

Data Availability Statement: Mention of trade names or commercial products in this publication is solely for the purpose of providing specific information and does not imply recommendation or endorsement by the USDA. USDA is an equal opportunity provider and employer.

Conflicts of Interest: The authors declare no conflict of interest.

References

1. Barringer, L.E.; Donovall, L.R.; Spichiger, S.-E.; Lynch, D.; Henry, D. The first new world record of *Lycorma delicatula* (Insecta: Hemiptera: Fulgoridae). *Entomol. News* **2015**, *125*, 20–23. [\[CrossRef\]](#)
2. Dara, S.K.; Barringer, L.; Arthurs, S.P. *Lycorma delicatula* (Hemiptera: Fulgoridae): A new invasive pest in the United States. *J. Integr. Pest Manag.* **2015**, *6*, 20. [\[CrossRef\]](#)
3. Center, N.I. Spotted Lanternfly Map. Available online: <https://www.stopslf.org/where-is-slf/slf-map/> (accessed on 22 November 2023).
4. Han, J.M.; Kim, H.; Lim, E.J.; Lee, S.; Kwon, Y.J.; Cho, S. *Lycorma delicatula* (Hemiptera: Auchenorrhyncha: Fulgoridae: Aphaeninae) finally, but suddenly arrived in Korea. *Entomol. Res.* **2008**, *38*, 281–286. [\[CrossRef\]](#)
5. Lee, D.-H.; Park, Y.-L.; Leskey, T.C. A review of biology and management of *Lycorma delicatula* (Hemiptera: Fulgoridae), an emerging global invasive species. *J. Asia-Pac. Entomol.* **2019**, *22*, 589–596. [\[CrossRef\]](#)
6. Barringer, L.; Ciafré, C.M. Worldwide feeding host plants of spotted lanternfly, with significant additions from North America. *Environ. Entomol.* **2020**, *49*, 999–1011. [\[CrossRef\]](#)
7. Liu, H. Oviposition substrate selection, egg mass characteristics, host preference, and life history of the spotted lanternfly (Hemiptera: Fulgoridae) in North America. *Environ. Entomol.* **2019**, *48*, 1452–1468. [\[CrossRef\]](#)
8. Cheetham, T. Pathological Alterations in Embryos of the Codling Moth (Lepidoptera: Tortricidae) Induced by Methyl Bromide. *Ann. Entomol. Soc. Am.* **1990**, *83*, 59–67. [\[CrossRef\]](#)
9. Mostafa, S.; Kamel, A.; El-Nahal, A.; El-Borollosy, F. Toxicity of carbon bisulphide and methyl bromide to the eggs of four stored product insects. *J. Stored Prod. Res.* **1972**, *8*, 193–198. [\[CrossRef\]](#)
10. Nitschke, K.; Albee, R.; Mattsson, J.; Miller, R. Incapacitation and treatment of rats exposed to a lethal dose of sulfuryl fluoride. *Fundam. Appl. Toxicol.* **1986**, *7*, 664–670. [\[CrossRef\]](#)
11. Mendrala, A.; Markham, D.; Eisenbrandt, D. Rapid uptake, metabolism, and elimination of inhaled sulfuryl fluoride fumigant by rats. *Toxicol. Sci.* **2005**, *86*, 239–247. [\[CrossRef\]](#)
12. Meikle, R.; Stewart, D.; Globus, O. Fumigant mode of action, drywood termite metabolism of Vikane fumigant as shown by labeled pool technique. *J. Agric. Food Chem.* **1963**, *11*, 226–230. [\[CrossRef\]](#)
13. Kim, K.; Lee, Y.H.; Kim, G.; Lee, B.-H.; Yang, J.-O.; Lee, S.-E. Ethyl formate and phosphine fumigations on the two-spotted spider mite, *Tetranychus urticae* and their biochemical responses. *Appl. Biol. Chem.* **2019**, *62*, 50. [\[CrossRef\]](#)
14. Haritos, V.; Dojchinov, G. Cytochrome c oxidase inhibition in the rice weevil *Sitophilus oryzae* (L.) by formate, the toxic metabolite of volatile alkyl formates. *Comp. Biochem. Physiol. Part C Toxicol. Pharmacol.* **2003**, *136*, 135–143. [\[CrossRef\]](#) [\[PubMed\]](#)
15. Nicholls, P. Formate as an inhibitor of cytochrome c oxidase. *Biochem. Biophys. Res. Commun.* **1975**, *67*, 610–616. [\[CrossRef\]](#)
16. Kim, K.; Lee, B.-H.; Park, J.S.; Yang, J.O.; Lee, S.-E. Biochemical mechanisms of fumigant toxicity by ethyl formate towards *Myzus persicae* nymphs. *J. Appl. Biol. Chem.* **2017**, *60*, 271–277. [\[CrossRef\]](#)
17. FAO. International Standards for Phytosanitary Measures (ISPM) No. 28. In *Phytosanitary Treatments for Regulated Pests*; FAO: Rome, Italy, 2007; pp. 3–11.
18. United Nations Environment Program. *Report of the Methyl Bromide Technical Options Committee (MBTOC)—2010 Assessment*; UNEP: Nairobi, Kenya, 2010.

19. Kenaga, E. Some biological, chemical and physical properties of sulfuryl fluoride as an insecticidal fumigant. *J. Econ. Entomol.* **1957**, *50*, 1–6. [\[CrossRef\]](#)
20. Reichmuth, C.S.M.; Dugast, J.-F.; Drinkall, M.J. On the efficacy of sulphuryl fluoride against stored product pest moths and beetles. In Proceedings of the Conference on Controlled Atmosphere and Fumigation in Stored Products, Nicosia, Cyprus, 21–26 April 1997.
21. United Nations Environment Program. *Special Review on Achieving Control of Pest Eggs by Sulfuryl Fluoride*; Report of the Technology and Economic Assessment Panel; UNEP: Nairobi, Kenya, 2011; pp. 110–136.
22. Walse, S.S.; Gautam, S.G.; Opit, G.P.; Margosan, D.; Tebbets, J.S. Sulfuryl fluoride-propylene oxide mixtures: Applications and efficacy. In Proceedings of the International Working Congress on Stored Product Protection, Chiang Mai, Thailand, 23 November 2014; Available online: <http://spiru.cgahr.ksu.edu/proj/iwcsp/iwcsp11.html> (accessed on 22 November 2023).
23. Baskin, S.I.; Brewer, T.G. *Cyanide Poisoning (From Medical Aspects of Chemical and Biological Warfare*; Frederick, R., Sidell, M.D., Ernest, T., Takafuji, M.D., Eds.; NCJ: Amsterdam, The Netherlands, 1997; pp. 271–286.
24. Sciuto, A.M.; Wong, B.J.; Martens, M.E.; Hoard-Fruchey, H.; Perkins, M.W. Phosphine toxicity: A story of disrupted mitochondrial metabolism. *Ann. New York Acad. Sci.* **2016**, *1374*, 41–51. [\[CrossRef\]](#)
25. Kashi, K.; Chefurka, W. The effect of phosphine on the absorption and circular dichroic spectra of cytochrome c and cytochrome oxidase. *Pestic. Biochem. Physiol.* **1976**, *6*, 350–362. [\[CrossRef\]](#)
26. Winks, R.; Waterford, C. The relationship between concentration and time in the toxicity of phosphine to adults of a resistant strain of *Tribolium castaneum* (Herbst). *J. Stored Prod. Res.* **1986**, *22*, 85–92. [\[CrossRef\]](#)
27. Walse, S.S.; Jimenez, L.R. Postharvest fumigation of fresh citrus with cylinderized phosphine to control bean thrips (Thysanoptera: Thripidae). *Horticulturae* **2021**, *7*, 134. [\[CrossRef\]](#)
28. Lampiri, E.; Agrafioti, P.; Athanassiou, C.G. Delayed mortality, resistance and the sweet spot, as the good, the bad and the ugly in phosphine use. *Sci. Rep.* **2021**, *11*, 1–16. [\[CrossRef\]](#)
29. Bond, E.J.; Dumas, T.; Hobbs, S. Corrosion of metals by the fumigant phosphine. *J. Stored Prod. Res.* **1984**, *20*, 57–63. [\[CrossRef\]](#)
30. Soderstrom, E.L.; Brandl, D.G.; Hartsell, P.L.; Mackey, B. Fumigants as treatments for harvested citrus fruits infested with *Asynonychus godmani* (Coleoptera: Curculionidae). *J. Econ. Entomol.* **1991**, *84*, 936–941. [\[CrossRef\]](#)
31. Bell, C. The tolerance of developmental stages of four stored product moths to phosphine. *J. Stored Prod. Res.* **1976**, *12*, 77–86. [\[CrossRef\]](#)
32. Su, N.-Y.; Scheffrahn, R.H. Efficacy of sulfuryl fluoride against four beetle pests of museums (Coleoptera: Dermestidae, Anobiidae). *J. Econ. Entomol.* **1990**, *83*, 879–882. [\[CrossRef\]](#)
33. Bell, C.; Savvidou, N. The toxicity of Vikane (sulfuryl fluoride) to age groups of eggs of the Mediterranean flour moth (*Ephestia kuehniella*). *J. Stored Prod. Res.* **1999**, *35*, 233–247. [\[CrossRef\]](#)
34. Baltaci, D.; Klementz, D.; Gerowitt, B.; Drinkall, M.; Reichmuth, C. Lethal effects of sulfuryl fluoride on eggs of different ages and other life stages of the warehouse moth *Ephestia elutella* (Hübner). *J. Stored Prod. Res.* **2009**, *45*, 19–23. [\[CrossRef\]](#)
35. Bonjour, E.; Opit, G.; Hardin, J.; Jones, C.; Payton, M.; Beeby, R. Efficacy of ozone fumigation against the major grain pests in stored wheat. *J. Econ. Entomol.* **2011**, *104*, 308–316. [\[CrossRef\]](#)
36. Athanassiou, C.G.; Phillips, T.W.; Aikins, M.J.; Hasan, M.M.; Throne, J.E. Effectiveness of sulfuryl fluoride for control of different life stages of stored-product psocids (Psocoptera). *J. Econ. Entomol.* **2012**, *105*, 282–287. [\[CrossRef\]](#)
37. Kenaga, E.E. Time, temperature and dosage relationships of several insecticidal fumigants. *J. Econ. Entomol.* **1961**, *54*, 537–542. [\[CrossRef\]](#)
38. Bell, C. Factors affecting the efficacy of sulphuryl fluoride as a fumigant. In Proceedings of the Ninth International Working Conference on Stored Product Protection, Sao Paulo, Brazil, 15–18 October 2006; pp. 519–526.
39. Outram, I. Factors affecting the resistance of insect eggs to sulphuryl fluoride—I: The uptake of sulphuryl-35S fluoride by insect eggs. *J. Stored Prod. Res.* **1967**, *3*, 255–260. [\[CrossRef\]](#)
40. Outram, I. Factors affecting the resistance of insect eggs to sulphuryl fluoride—II: The distribution of sulphuryl-35S fluoride in insect eggs after fumigation. *J. Stored Prod. Res.* **1967**, *3*, 353–358. [\[CrossRef\]](#)
41. Gautam, S.; Opit, G.; Margosan, D.; Tebbets, J.; Walse, S. Egg morphology of key stored-product insect pests of the United States. *Ann. Entomol. Soc. Am.* **2014**, *107*, 1–10. [\[CrossRef\]](#)
42. Gautam, S.; Opit, G.; Margosan, D.; Hoffmann, D.; Tebbets, J.; Walse, S. Comparative egg morphology and chorionic ultrastructure of key stored-product insect pests. *Ann. Entomol. Soc. Am.* **2015**, *108*, 43–56. [\[CrossRef\]](#)
43. Hinton, H.E. Respiratory systems. *Biol. Insect Eggs* **1981**, *1*, 95–148.
44. Trougakos, I.P.; Margaritis, L.H. Novel morphological and physiological aspects of insect eggs. In *Chemoecology of Insect Eggs and Egg Deposition*; Blackwell Publishing: Berlin, Germany, 2003; pp. 2–36.
45. Kučerová, Z.; Stejskal, V. Comparative egg morphology of silvanid and laemophloeid beetles (Coleoptera) occurring in stored products. *J. Stored Prod. Res.* **2002**, *38*, 219–227. [\[CrossRef\]](#)
46. Bozzola, J.J.; Russell, L.D. *Electron Microscopy: Principles and Techniques for Biologists*; Jones & Bartlett Learning: Burlington, MA, USA, 1999.
47. Hayat, M.A. *Principles and Techniques of Electron Microscopy: Biological Applications*, 4th ed.; Cambridge University Press: Cambridge, UK, 2000; 543p.

48. Matesco, V.C.; Fürstenau, B.; Bernardes, J.L.; Schwertner, C.F.; Grazia, J. Morphological features of the eggs of Pentatomidae (Hemiptera: Heteroptera). *Zootaxa* **2009**, *1984*, 1–30. [[CrossRef](#)]
49. Matesco, V.C.; Bianchi, F.M.; Fürstenau, B.B.R.J.; Da Silva, P.P.; Campos, L.A.; Grazia, J. External egg structure of the Pentatomidae (Hemiptera: Heteroptera) and the search for characters with phylogenetic importance. *Zootaxa* **2014**, *3768*, 351–385. [[CrossRef](#)]
50. Javahery, M. Development of eggs in some true bugs (Hemiptera–Heteroptera). Part I. Pentatomoidea. *Can. Entomol.* **1994**, *126*, 401–433. [[CrossRef](#)]
51. Vilimova, J.; Rohanova, M. The external morphology of eggs of three Rhopalidae species (Hemiptera: Heteroptera) with a review of the eggs of this family. *Acta Entomol. Musei Natl. Pragae* **2010**, *50*, 75–95.
52. Arbogast, R.T.; Lecato, G.L.; Van Byrd, R. External morphology of some eggs of stored-product moths (Lepidoptera Pyralidae, Gelechiidae, Tineidae). *Int. J. Insect Morphol. Embryol.* **1980**, *9*, 165–177. [[CrossRef](#)]

Disclaimer/Publisher’s Note: The statements, opinions and data contained in all publications are solely those of the individual author(s) and contributor(s) and not of MDPI and/or the editor(s). MDPI and/or the editor(s) disclaim responsibility for any injury to people or property resulting from any ideas, methods, instructions or products referred to in the content.